Squeezing Oscillations in a Multimode Bosonic Josephson Junction

Tiantian Zhang,* Mira Maiwöger, Filippo Borselli, Yevhenii Kuriatnikov, Jörg Schmiedmayer, and Maximilian Prüfer†

Vienna Center for Quantum Science and Technology, Technische Universität Wien, Atominstitut, Vienna, Austria

(Received 17 April 2023; revised 21 December 2023; accepted 9 February 2024; published 15 March 2024)

Quantum simulators built from ultracold atoms promise to study quantum phenomena in interacting many-body systems. However, it remains a challenge to experimentally prepare strongly correlated continuous systems such that the properties are dominated by quantum fluctuations. Here, we show how to enhance the quantum correlations in a one-dimensional multimode bosonic Josephson junction, which is a quantum simulator of the sine-Gordon field theory. Our approach is based on the ability to track the nonequilibrium dynamics of quantum properties. After creating a bosonic Josephson junction at the stable fixed point of the classical phase space, we observe squeezing oscillations in the two conjugate variables. We show that the squeezing oscillation frequency can be tuned by more than one order of magnitude, and we are able to achieve a spin squeezing close to 10 dB by utilizing these oscillatory dynamics. The impact of improved spin squeezing is directly revealed by detecting enhanced spatial phase correlations between decoupled condensates. Our work provides new ways for engineering correlations and entanglement in the external degree of freedom of interacting many-body systems.

DOI: 10.1103/PhysRevX.14.011049

Subject Areas: Atomic and Molecular Physics, Quantum Physics

I. INTRODUCTION

Understanding the role of quantum fluctuations and entanglement in interacting many-body systems is of critical importance for the development of quantum technologies, such as quantum metrology [1,2] and quantum simulation [3]. In particular, the ability to prepare entanglement [4] in quantum many-body systems is pivotal. In this context, ultracold atoms have proven to be a versatile platform [1].

Internal spin degrees of freedom (d.o.f.) offer a high level of control, and using a single spatial mode spin-squeezed states could be generated experimentally [5–8]. Creating entangled quantum states in motional d.o.f., for example, in tunnel-coupled BECs in double wells (DWs) [9,10], is, on the contrary, less explored; the impact of spin squeezing and entanglement has only been studied with respect to the global observables.

For spatially extended systems, where more than one longitudinal mode is occupied, the interplay between transverse (spin) and longitudinal d.o.f. leads to new physical phenomena. For coupling internal states, interesting dynamical phenomena as well as a high degree of control have been shown [11,12]; for tunnel-coupled systems, the influence of the multimode situation on Josephson oscillations has been studied [13]. However, so far the quantum regime has not been accessible.

Interestingly, in the one-dimensional (1D) regime these systems are excellent quantum simulators for the sine-Gordon field theory [14,15], which was mainly explored in tunnel-coupled systems [16,17]. It is worth pointing out that BECs in DWs at equilibrium can be experimentally achieved by direct cooling in DWs [16]. But fluctuations introduced by the finite temperature make it challenging to prepare the system in the quantum correlated regime [18]. However, it has been shown that using a splitting routine from a single condensate, quantum correlated states can be prepared in a multimode scenario [10]. In this work, we combine the ability to prepare quantum correlated states with spatially resolved measurements of the sine-Gordon fields entering a new regime.

We realize a multimode bosonic Josephson junction (BJJ) [19,20] by splitting 1D quasi-BECs into a DW (see Fig. 1, upper panel). Instead of studying Josephson oscillations [13,21–25], we prepare the system at the stable fixed point of the classical phase space and access its quantum properties. Despite the stationary expectation values of both relevant observables, relative number and

*Corresponding author: tiantian.zhang@tuwien.ac.at
†Corresponding author: maximilian.pruefer@tuwien.ac.at

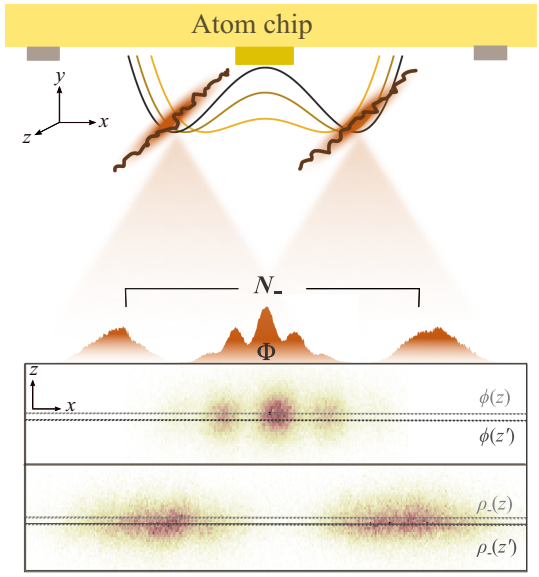

FIG. 1. System and readout with spatial resolution. Two 1D quasi-BECs with locally fluctuating quantum phases trapped magnetically below an atom chip with rf dressing technique. The local relative phase $\phi(z)$ and relative atom density $\rho_-(z)$ between the two BECs are detected with fluorescence imaging after a long time of flight. The spatial resolution allows us to probe the spatial phase correlations along the condensates. We integrate over the longitudinal direction to obtain the global observables, namely the relative phase Φ and relative atom number N_-.

relative phase, we observe oscillatory dynamics of the quantum fluctuations which result from the evolution of an initial quantum state different from the ground state at zero temperature. We employ these nonequilibrium dynamics of the fluctuations in the BJJ to foster strong spin squeezing in decoupled condensates. Furthermore, we study its impact on spatial phase correlations in the multimode system.

To probe the multimode properties of the prepared states we use a spatially resolved detection of the relative phase (see Fig. 1, lower panel). The observations in this observable enable us to demonstrate how the improved number squeezing enhances spatial correlations between two decoupled 1D condensates. We are able to connect quantum properties resulting from the preparation process to enhanced phase correlations in a regime where a sine-Gordon model is realized. The enhanced squeezing can in principle be directly related to lower effective temperatures in the prethermalized regime [26,27], and our work thus shows a pathway to prepare sine-Gordon field simulators in a regime dominated by quantum fluctuations.

II. REALIZATION AND READOUT OF A MULTIMODE BJJ

We realize a multimode BJJ with 1D tunnel-coupled quasi-BECs of ^{87}Rb atoms trapped magnetically under an atom chip [28]. The DW potential is generated with the radio-frequency (rf) dressing [29] technique. The dressing is calibrated such that the precise transformation from a single well to a DW is achieved by ramping up the amplitude $\mathcal{A}$ of the rf field whose value is normalized to the maximal current. We display in Fig. 1 the transverse trap configuration and typical experimental readout with our single-atom-sensitive fluorescence imaging system [30] after time of flight of $t_F = 43.4$ ms. The aspect ratio between the radial and axial trap frequency is $\sim$100.

Each of the quasicondensates in a DW can be described in the density-phase representation by $\Psi_j = \sqrt{\rho_j(z)}\exp[-i\phi_j(z)]$, where $j \in [L, R]$ labels the left (L) and the right (R) condensate. The local density ρ_j and local phase ϕ_j are spatially varying and fluctuating fields. This is illustrated by the wiggly brown lines in Fig. 1. We are interested in the local fields in the relative d.o.f., namely the local relative density $\rho_-(z) = \rho_R(z) - \rho_L(z)$ and local relative phase $\phi(z) = \phi_R(z) - \phi_L(z)$. For finitely tunnel-coupled condensates, the spatially dependent relative phase field $\phi(z)$ can be described by the sine-Gordon field theory [14].

Our imaging allows us to measure the relative phase with spatial resolution (see Fig. 1, lower panel). From this, we can access the two-point phase correlations to study the sine-Gordon physics in the multimode regime, as will be discussed later. Valuable insights into the dynamical quantum properties of BJJs can already be obtained from a single-mode description of the BJJ [31]. Therefore, we will first investigate the properties of the two global observables of the 1D BJJ, the relative atom number, $N_- = \sum_z \rho_-(z)$, and the relative phase, $\Phi = \sum_z \phi(z)$, which correspond to the spatial zeroth mode.

The macroscopic dynamics of the global observables N_- and Φ in a BJJ can be described by the two-mode Bose-Hubbard (BH) model,

$$\mathcal{H} = \frac{2J}{\hbar}\left[\frac{UN}{4J}n^2 - \sqrt{1-n^2}\cos\Phi\right], \tag{1}$$

where $N = N_L + N_R$ is the total atom number, $n = N_-/N$ is the relative imbalance, U is the interaction strength, and J is the single particle tunnel coupling strength. The Josephson regime of the BJJ is indicated by $1/N \ll U/2J \ll N$. From Eq. (1), we can obtain the Josephson oscillation frequency [19,20] of the mean values $\langle\Phi\rangle$ and $\langle N_-\rangle$,

$$f_p = \frac{2J}{h}\sqrt{\langle\cos\Phi_0\rangle + \frac{UN}{2J}}, \tag{2}$$

also known as the plasma frequency. Here $\cos\Phi_0$ indicates the initial phase coherence factor. From Eq. (2), we see that f_p depends explicitly on the single particle tunnel coupling strength J.

For the multimode many-body dynamics dominating in decoupled DWs, the two-mode BH model definitely does not give a full description. However, we will see in the following that it nicely captures the dynamics of the squeezing in the spatial zeroth mode. Exact modeling of the splitting process together with the ensuing dynamics are challenging when taking into account the true multimode quantum dynamics; thus, quantum simulations can provide new insights.

III. PREPARING QUANTUM CORRELATED STATES

To prepare strongly correlated BECs, we split a single BEC into two by transforming a single well into a DW [see Fig. 2(a)]. BEC splitting as a pathway to generate quantum correlated states was investigated in many earlier works [9,32,33]; here, we introduce and implement a new scheme which is based on understanding the nonequilibrium dynamics after a nonadiabatic splitting into a tunnel-coupled DW. In the following, we introduce the relevant quantities and summarize our findings which lay the basis for observing the nonequilibrium dynamics of the prepared squeezed state.

To quantify the fluctuations of the observables, we define the squeezing factors,

$$\xi_N^2 = \frac{\Delta^2 N_-}{N}, \qquad \xi_\Phi^2 = \Delta^2\Phi \cdot N, \tag{3}$$

where $\Delta^2 N_-$ and $\Delta^2\Phi$ represent the statistical variance, evaluated as in Fig. 8. We use the quadrature projection noise of spin coherent states in the denominators. Hence, $\xi_N^2 = \xi_\Phi^2 = 1$ represents the standard quantum limit (SQL). Furthermore, spin-squeezed states [34,35] representing a class of entangled states are characterized by spin squeezing factor $\xi_s^2 = \xi_N^2/\langle\cos\Phi\rangle^2 < 1$, where $\langle\cos\Phi\rangle$ is the phase coherence factor.

The ground state of the many-body Hamiltonian [36] exhibits a growing degree of number squeezing in less coupled DWs owing to repulsive interatomic interactions. In Fig. 2(a), we show the experimentally inferred squeezing factors in N_- and Φ as a result of BEC splitting with finite duration, denoted with rescaled rf dressing amplitude $\mathcal{A}$. We conduct ∼200 repetitions for each measurement to ensure reliable statistics. At the beginning of the Josephson

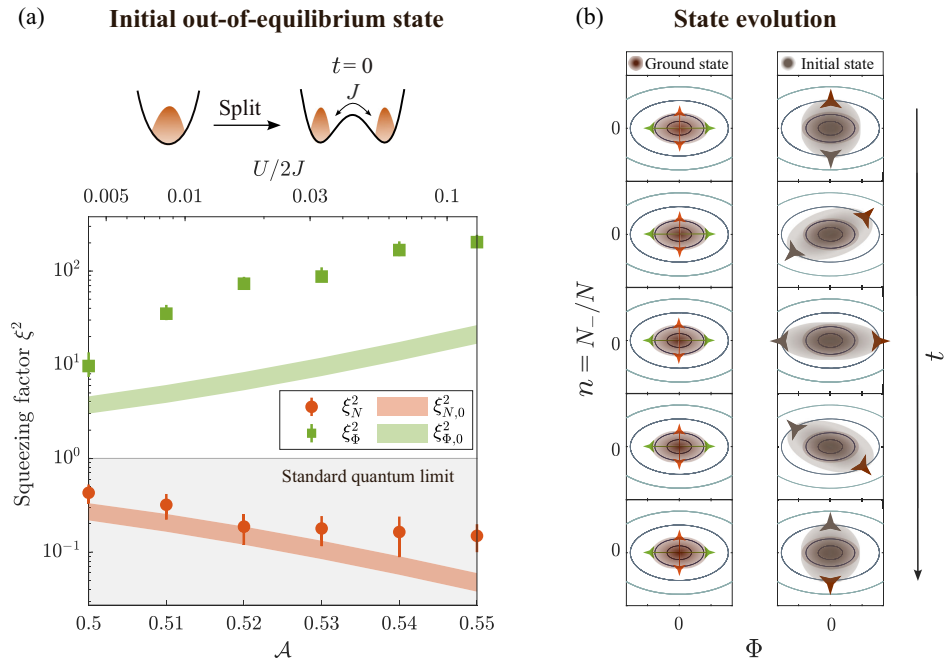

FIG. 2. Preparation and dynamics of spin-squeezed quasi-BECs in the Josephson regime. (a) Measured squeezing factors in N_- and Φ quadrature, denoted as ξ_N^2 and ξ_Φ^2, right after a linear ramp-up at a constant ramp speed to various tunnel-coupled DWs, denoted with the rescaled rf dressing amplitude $\mathcal{A}$. In the upper x axis, the parameter $1/N \ll U/2J \ll N$ indicates that we are in the Josephson regime of BJJ. The colored bands mark the expected ground state squeezing factors of BJJ at zero temperature [Eq. (A3)] with atom number $N \in [2, 5] \times 10^3$. (b) Schematics of state evolution in the classical phase space. Left-hand column illustrates the expected ground state fluctuation of BJJ according to Eq. (A4), where orange (green) arrows represent projection noise in the relative number (phase) quadrature. The right-hand column represents the out-of-equilibrium quantum state evolution. The triangle markers indicate single classical realizations orbiting along the equipotential lines at the plasma frequency f_p. In the Josephson regime, the distribution of out-of-equilibrium states rotates and deforms, which results in squeezing oscillations. A full period of the quantum state evolution around the stable fixed point ($n = N_-/N = 0$ and $\Phi = 0$) conforms to a half period of evolution of single realizations (mean values) in the phase space.

regime, $U/2J \sim 1/N$, the measured relative number fluctuations of split BECs approach the expected ground state number squeezing $\xi^2_{N,0}$ [see Appendix Eq. (A4)].

During further ramp-up of the rf amplitude $\mathcal{A}$, the adiabaticity condition can no longer be satisfied. This breakdown is shown explicitly in Fig. 2(a), where ξ^2_N become increasingly larger than $\xi^2_{N,0}$ in less tunnel-coupled DWs. This initialized out-of-equilibrium state with BEC splitting is expected to evolve dynamically in the Josephson regime [see Fig. 2(b)]. As we will discuss in the following sections, this evolution of the quantum state in phase spaces with number-squeezed ground states is not just a rotation, but also additional shearing.

The fluctuations in the relative phase are always much above the expected ground state phase squeezing factor $\xi^2_{\Phi,0}$, as shown in Fig. 2(b). This is due to the interatomic interaction induced phase diffusion [37] during the ramp and can be prevented by increasing the splitting speed of linear ramps. The trade-off of faster splitting is poorer number squeezing right after the splitting. Thus, alternative splitting routines beyond linear single ramps are sought after to enhance spin squeezing in decoupled traps.

IV. SQUEEZING OSCILLATIONS IN CONJUGATE QUADRATURES

We prepare two BECs in a strongly coupled DW ($\mathcal{A} = 0.5$) by linearly ramping up from a single well; this prepares the system at the stable fixed point of the classical phase space, i.e., $\langle N_- \rangle = 0$ and $\langle \Phi \rangle = 0$ (see Fig. 10) with phase space fluctuations different from the ground state. By tracking the evolution of this out-of-equilibrium quantum state in the strongly coupled double well, we observe the dynamics of the quantum fluctuations of the conjugate observables (see Fig. 3).

The squeezing factors in both quadratures undergo oscillatory dynamics. Strikingly, the number quadrature stays always squeezed while the phase never gets squeezed below the SQL; i.e. the oscillatory dynamics is not a simple linear rotation of the state in phase space. This results from the interplay of tunnel coupling and on-site interaction and leads to a rotation and deformation of the state [see Figs. 2(b) and 3, inset]. We can understand the frequency of the oscillation with the intuitive picture that a π rotation of a single realization corresponds to a 2π rotation of quantum state distribution in phase space [see Fig. 2(b) and the Appendix]. We thereby deduce that the squeezing oscillations are twice as fast as the Josephson oscillations of the mean (with plasma frequency f_p); this is in accordance with a semiclassical analysis for Raman coupled BECs [38].

We fit the observed squeezing factors in Fig. 3 with a sine function to determine the squeezing oscillation frequency and obtain $f_\xi = 567(29)$ Hz in relative number N_- quadrature with total atom number $N = 4154(35)$ and

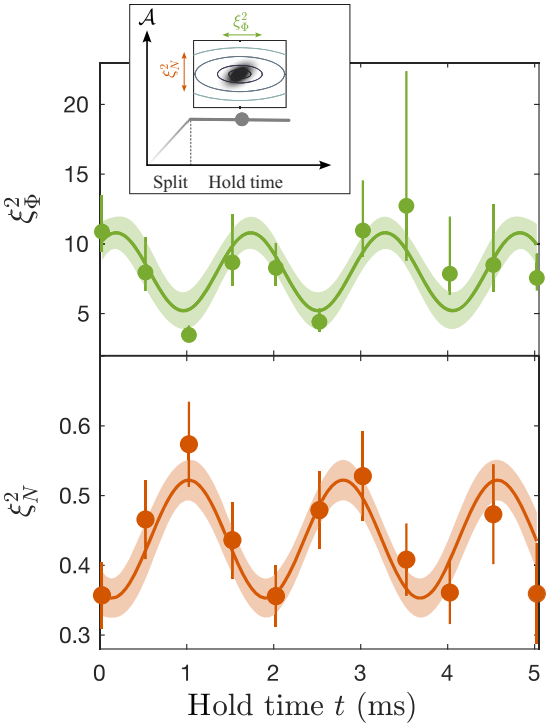

FIG. 3. Squeezing oscillations in a coupled double well. (a) Dynamics of the fluctuations of relative phase (green) and relative number (orange markers) for variable hold time in the coupled trap after the splitting. We observe oscillatory dynamics with comparable frequency and relative phase shift of π. The oscillatory dynamics is not a simple linear rotation of the state in phase space but results from the interplay of tunnel coupling and on-site interaction and leads to a rotation plus deformation of the state (see inset). From a sinusoidal fit (solid lines) we extract the frequencies which are roughly twice the plasma frequency as expected from the rotation and shearing of the distribution in the phase space [see inset and Fig. 2(b)]. Bands indicate 68% prediction confidence interval of the fits and error bars represent one standard error of the mean.

$f_\xi = 649(33)$ Hz in relative phase Φ quadrature with $N = 4302(45)$ (see the Appendix). The measured squeezing oscillations in both quadratures as expected from the nonlinear Josephson dynamics match with twice the experimentally measured plasma frequency f_p and have a π phase shift with respect to each other. Combining the complementary measurements in Fig. 3, we infer the mean quantum state fluctuations in the phase space to be $\overline{\xi^2_N} \cdot \overline{\xi^2_\Phi} \approx 3.5$ with $\overline{\xi^2_N} = 0.44(2)$ and $\overline{\xi^2_\Phi} = 8.0(7)$.

V. TWO-STEP SEQUENCE FOR OPTIMIZED SPIN SQUEEZING

So far, mostly simple linear ramps have been used to generate squeezing. In single-mode situations theoretical studies showed that nonlinear ramps generated by optimal control can lead to better squeezing [39,40]; for our multimode BJJ the development of a many-body

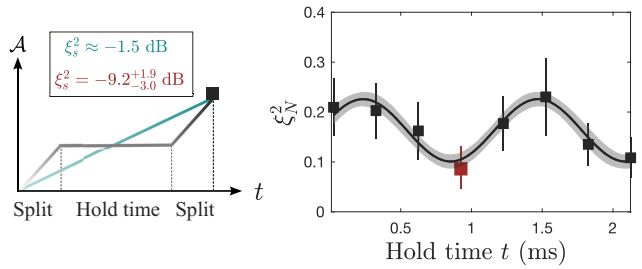

FIG. 4. Two-step sequence for optimized spin squeezing. For optimizing the spin squeezing in the decoupled trap ($\mathcal{A} = 0.65$), we perform a two-step sequence (black line in left-hand schematic) instead of a simple linear ramp (blue line). By varying the hold time in the coupled trap ($\mathcal{A} = 0.5$) and performing the final measurement after adding a second linear ramp to the decoupled trap, we observe an oscillatory behavior. This oscillation is similar to Fig. 3, but overall better number squeezing. For the optimal spin-squeezed point (red marker) we find −9.2 dB spin squeezing instead of −1.5 dB for a single linear ramp with a similar total duration as the two-step sequence.

simulation, required for performing open loop optimization on spin squeezing, is not possible, as the splitting process is hard to calculate. Thus we develop an experimentally tractable two-step approach (see Fig. 4) based on the observed squeezing oscillations in the coupled DW; in single-mode spinor BECs a similar approach has been used to achieve spin-squeezed ground states [41,42]. Here, we employ it for optimizing the spin squeezing in a decoupled DW ($J = 0$) in a multimode situation (see Fig. 4). It is of particular interest to use entangled BECs in a decoupled DW as a sensitivity-enhanced matter-wave interferometer [1,2,10].

We show in Fig. 4 that the generated squeezing oscillation in the coupled DW is successfully preserved after the ramp to the decoupled DW with two-step splitting; this means we are able to manipulate the quantum properties in the decoupled trap by a holding time in the coupled trap. Furthermore, the number squeezing is even further enhanced during the second ramp. With this approach, we obtain a phase coherence factor of $\langle \cos \Phi \rangle = 0.86^{+0.01}_{-0.02}$. This leads to a spin squeezing factor [5] of $\xi_s^2 = -9.2^{+1.9}_{-3.0}$ dB [with no detection noise correction, $\xi_s^2 = -4.0(1.1)$ dB; see the Appendix], which witnesses many-body entanglement [35].

In contrast, a single linear ramp with a similar duration yields lower spin squeezing of $\xi_s^2 \approx -1.5$ dB, demonstrating a significant gain with two-step splitting. A simple way to understand this is that two-step splitting enables us to achieve optimal number squeezing at an earlier stage of the splitting procedure and, as a result, suppressing the phase diffusion more efficiently.

VI. TUNING SQUEEZING OSCILLATIONS

To achieve controlled preparation of strongly correlated states with two-step splitting, it is crucial to understand the control parameters and tunability of the squeezing oscillation frequency. We identify two strategies: the first one involves tuning the parameters in a static BJJ, and the second one involves introducing time dependence on the control parameters through transversal motions.

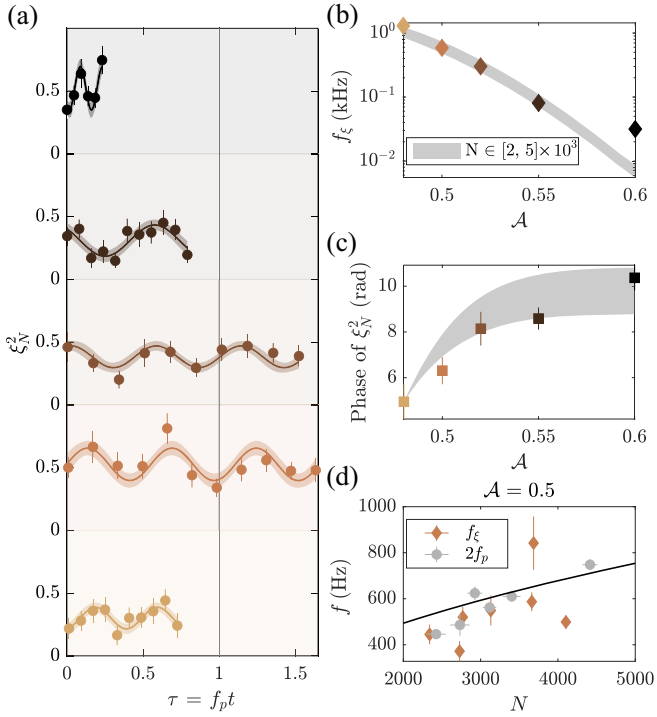

FIG. 5. Tuning squeezing oscillation frequency. (a) Observed number squeezing factor ξ_N^2 evolution in coupled DWs after a constant splitting speed with increasing $\mathcal{A}$ (bottom to top). The solid line is a fitted sine function with 68% simultaneous prediction bounds. (b) The extracted squeezing frequency f_ξ (diamond) from (a) together with the calculated prediction $2f_p$ (gray shade) with $N \in [2, 5] \times 10^3$. (c) Fitted initial phases of squeezing oscillations in (a) compared to the expected accumulated phases (gray band) of the quantum state during the linear ramp with constant ramp speed to different DWs at $\mathcal{A}$ with atom number $N \in [2, 5] \times 10^3$ as in (b). Here the band uses the fitted phase of squeezing oscillation at $\mathcal{A} = 0.48$ [in (a)] as the initial value. (d) Dependence of f_ξ (diamond) on total atom number N in coupled DW at $\mathcal{A} = 0.5$, and for comparison experimentally measured plasma frequency $2f_p$ (circle) and solid line marks the inferred $2f_p$ from Eq. (2).

We explore experimentally the frequency scaling in elongated BJJ based on Eq. (2). In Fig. 5(a), we show the measured number squeezing oscillations in different DWs with decreasing single particle tunnel coupling J (bottom to top). We observe squeezing oscillations with frequencies spanning more than one order of magnitude. In Fig. 5(b), we plot collectively the extracted frequencies and as a comparison the expectation of $2f_p$ (gray band) estimated directly from Eq. (2). Here, J for each $\mathcal{A}$ is inferred from simulated DW potential and experimental atom number $N \in [2, 5] \times 10^3$. We find good agreement

between the experimentally observed fluctuation dynamics on the global observable N_- (zeroth mode) of the multimode BJJ and the simple calculations based on the two-mode BH model. This confirms first of all that the observed squeezing oscillations indeed originate from stationary nonlinear Josephson dynamics.

On top of which, we show in Fig. 5(c) that fitted phases of the squeezing oscillations in Fig. 5(a) match quantitatively with the expected evolution of the quantum state during the linear ramp. The experimental results in Fig. 5(a) are obtained after single linear ramps with the same splitting speed. We can estimate the additionally gained phase during the ramp compared to the first experimental data point at $\mathcal{A} = 0.48$ (set as $t = 0$) as the sum of constantly evolving plasma frequencies $f_p(t_i)$ [Eq. (2)] over a ramp time ΔT, namely $\Delta T \cdot \sum_{t=0}^{\Delta T} 2\pi f_p(t)$. Despite the quantum state evolution in the phase space [Fig. 2(b)] not being a simple rotation, the differences between the initial phases in different DWs built up during the ramp can be surprisingly well predicted with this simple estimation.

The other d.o.f. for tuning squeezing oscillation is the total atom number N. In Fig. 5(c) we show experimentally measured squeezing oscillation frequency f_ξ as a function of N (for fixed $\mathcal{A} = 0.5$) and compare them directly with experimentally measured plasma frequency $2f_p$ and a solid line derived from Eq. (2). In this strongly coupled DW, we can tune squeezing oscillation frequency from 300 to 800 Hz by adjusting only the atom number.

To expand the tuning capabilities, we incorporate an active modulation on the tunneling mechanism. By performing a splitting quench, we excite out-of-phase transverse sloshing between the two BECs at the transverse trap frequency $f_x = 1418(10)$ Hz. We depict in Fig. 6(a) this induced motion with the inferred intercondensate distance d. This motional excitation drives the effective tunnel coupling J periodically at the trap frequency f_x. We show in Fig. 6(b) how this periodic drive enforces ξ_N^2 to oscillate at frequencies comparable with f_x. Furthermore, we can reproduce this oscillation frequency with a two-step splitting quench to the decoupled DW [see Fig. 6(c)].

By utilizing this method, we boost the preparation of spin-squeezed states with two-step sequence from two perspectives: reduced ramp times and faster squeezing dynamics. Our observations potentially facilitate investigations into captivating phenomena like parametric resonance [43] and Floquet engineering [44].

VII. SQUEEZING-PROTECTED SPATIAL CORRELATIONS

With the gained insight on how to optimize spin squeezing, we now investigate how the spin squeezing influences the spatial correlations in our multimode system which is a quantum simulator for the sine-Gordon field theory. In a decoupled DW, number squeezing prolongs the

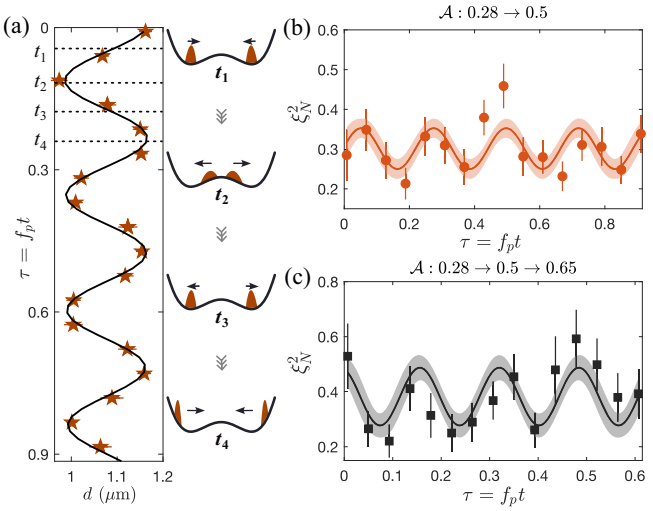

FIG. 6. Driving number squeezing oscillation. (a) Intercondensate distance d in 0.5 trap resulting from splitting quench with $\kappa = 0.085$ ms^{-1} into $\mathcal{A} = 0.5$ trap. d oscillates at the transverse trap frequency f_x. With this effective periodic modulation of tunnel coupling, we observe in (b) that ξ_N^2 (orange circle) is driven at the trap frequency $f_x > f_p$. (c) Transferred squeezing oscillation after a two-step quench. τ indicates hold time in coupled DW.

global phase coherence by reducing the relative phase diffusion [10,33]. Indeed, we find a good qualitative agreement between experimentally extracted global phase diffusion rates and the levels of global number squeezing (see Fig. 13).

The spatial resolution of our imaging system grants direct access to the local relative phase (see the Appendix). This allows us to explore how the observed number squeezing impacts the local dephasing [26,45]. To study this, we prepare split BECs in an effectively decoupled DW, with two different levels of (global) number squeezing. We consider the two-point phase correlation function (PCF), defined as $\langle \cos \theta(z, z') \rangle$, where $\theta(z, z') = \phi(z) - \phi(z')$ is the relative phase field.

In Fig. 7(a), we compare the two-point PCF in the decoupled DW at two time instances, $t = 0$ ms and $t = 4$ ms, after initial preparation with $\xi_N^2 = 0.31(3)$ (upper panels) and 0.44(4) (lower panels). Despite higher PCF in the beginning, the decay is faster with weaker number squeezing (lower panels). For better visualization, we plot in Fig. 7(b) the averaged PCF, $\langle \cos \theta(\bar{z}) \rangle$, where $\bar{z} = |z - z'|$, in the central region $z = [-36, 36]$ μm. It is evident that enhanced global number squeezing slows down the decay of PCF over large spatial separations $\bar{z}$.

For prethermalized states [27], it was found that the local number squeezing is directly linked to the effective temperature T^- of the implemented sine-Gordon model according to the relation $T^- \propto \xi_N^2$ (see Ref. [46] and the Appendix); thus, for decoupled DWs enhanced squeezing leads to a larger phase coherence length $\lambda_T \propto 1/T^-$.

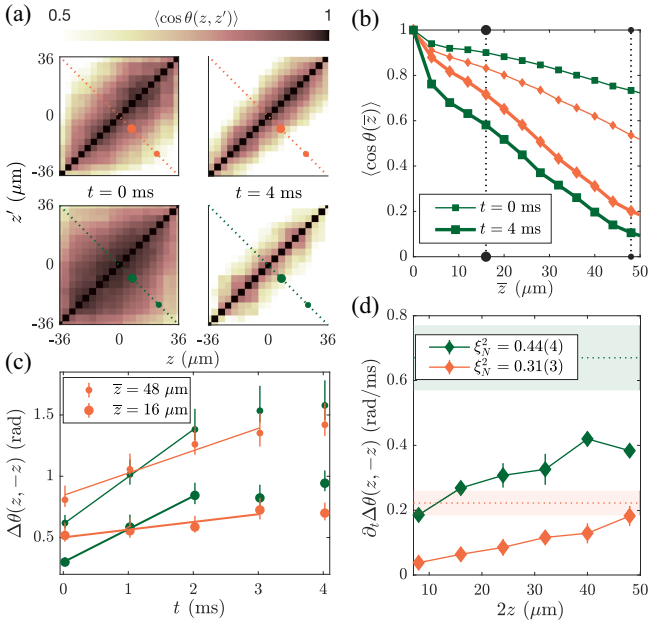

FIG. 7. Influence of number squeezing on multimode phase correlation function. (a) Phase correlation function (PCF) $\langle\cos\theta(z,z')\rangle$ between two spatial positions z and z' along the condensates. Upper and lower panels show PCF of a state with 0.31(3) (orange) and $\xi_N^2 = 0.44(4)$ (green) and at time t after splitting to DW at $\mathcal{A} = 0.6$. (b) Spatially averaged PCF, $\langle\cos\theta(\bar{z})\rangle$, with $\bar{z} = |z - z'|$ from (a) visualizes how number squeezing suppresses decay of PCF. (c) Evolution of $\Delta\theta(z,-z)$ for $z = 8$ μm (big circle) and $z = 24$ μm (small circle). We infer the dephasing rate $\partial_t\Delta\theta(z,-z)$ with a linear fit and plot the extracted rates in (d) (see Fig. 14 for all distances z). The shaded regions represent the extracted global phase diffusion rate. We observe a spatial dependence of $\partial_t\Delta\theta(z,-z)$ along the condensates, which hints at local number squeezing originating from the multimode dynamics of quasicondensates.

In multimode systems, different spatial modes can in principle feature different levels of squeezing; this would result in mode-dependent effective temperatures as, for example, in a generalized Gibbs ensemble [47]. To examine the spatial dependence of squeezing in our experiment, we track the time evolution of the fluctuations $\Delta\theta(z,-z)$ of the relative phase field between two symmetric points. We extract linear rates $\partial_t\Delta\theta(z,-z)$ and show an exemplary at two distances $z = 8$ and 24 μm in Fig. 7(c) (see Fig. 14 for dephasing rates at more distances). We observe a spatial dependence of dephasing rates $\partial_t\Delta\theta(z,-z)$ [see Fig. 7(d)]. As expected, the experimental set with better global number squeezing yields an overall lower dephasing rate $\partial_t\Delta\theta(z,-z)$, and additionally we observe slower dephasing at small distances.

VIII. CONCLUSION AND OUTLOOK

We have observed oscillatory dynamics of quantum fluctuations on conjugate variables of a multimode BJJ and, based on this observation, developed a more efficient approach for achieving enhanced spin-squeezed states. We envision a more efficient preparation of spin-squeezed states with the help of optimal control algorithms optimizing the classical external dynamics after rapid two-step sequences. In consideration of our 1D multimode system, we have demonstrated the influence of number squeezing on prohibiting local dephasing in decoupled DWs. In the future, the ability to track the squeezing dynamics provides a new way for optimizing the preparation of strongly correlated sine-Gordon field simulators with lower effective temperatures; by experimentally approaching a regime that is dominated by quantum fluctuations, measurements of the entanglement entropy in quantum fields will become possible [48].

Source data and all other data that support the plots within this paper and other findings of this study are available from the corresponding authors upon reasonable request.

ACKNOWLEDGMENTS

We thank Sebastian Erne, Camille Lévêque, and Igor Mazets for discussions and Philipp Kunkel for comments on the manuscript. This work is supported by the DFG/FWF CRC 1225 "ISOQUANT" [Austrian Science Fund (FWF) P 36236] and the QUANTERA project MENTA (FWF: I-6006). M. P. has received funding from the European Union's Horizon 2020 research and innovation program under the Marie Skłodowska-Curie Grant Agreement No. 101032523.

T. Z. and M. P. took the experimental data with the help of Y. K., M. M., and F. B. T. Z. analyzed the data with the help of M. P. T. Z., Y. K., J. S., and M. P. discussed the experimental findings and wrote the manuscript with input from all authors. J. S. and M. P. supervised the work.

The authors declare no competing financial interests.

APPENDIX

1. Number squeezing factor estimation

By summing up the total photon signal of each cloud (see Fig. 1) to obtain S_L and S_R, we can calculate the global number squeezing factor using,

$$\xi_N^2 = \frac{\Delta^2 S_- - 2S - 2\Delta^2 b}{\bar{p}S}. \tag{A1}$$

Here $\Delta^2 S_- = \Delta^2(S_L - S_R)$ is the variance on the relative photon signal, $\bar{p}$ is the experimentally calibrated average number of photons collected per atom, and $\Delta^2 b$ is the variance of the background noise of an atom-free region on the electron multiplying charge-coupled device (EMCCD) chip. The noise of $2S = 2(S_L + S_R)$ originates

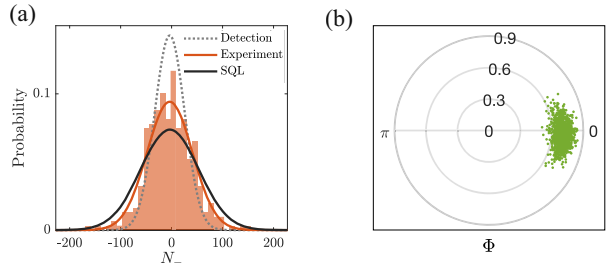

FIG. 8. Statistical evaluation of distribution. (a) Histogram of N_- together with fitted normal distribution (orange). As a reference, we show a binomial distribution (black, indicating the standard quantum limit) and a normal distribution with the width corresponding to the detection noise level (gray). (b) Polar distribution of Φ with fringe visibility C as radii. Error bars represent one standard error of the mean.

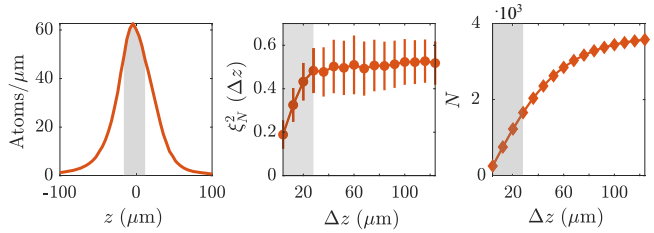

FIG. 9. Imaging influence on spatially resolved number squeezing detection. Left: longitudinal profile of BEC. Middle: influence of finite integration length Δz on evaluation of number squeezing factor ξ_N^2. Δz is evaluated symmetrically around the peak density along the condensate. Right: atom number N within integration region Δz. The shaded region indicates the lower bound of Δz for reliable estimation of ξ_N^2.

from the electron multiplication process of the EMCCD chip. $2S + \Delta^2 b$ is the combined detection noise which is indicated as gray dotted line (Gaussian with corresponding width) in the histogram of N_- in Fig. 8(a).

2. Extraction of relative phase

We fit the interference fringe slicewise with $\rho(x) \approx g(x)\{1 + C\cos[k_0(x - x_0) + \phi]\}$ to extract the local relative phase ϕ and the fringe visibility C, indicating the single particle coherence. To minimize the readout error originating from the locally fluctuating relative phases, we extract the global relative phase $\Phi = \arg\{\overline{\exp[i\phi(z)]}\}$, based on independently fitted local relative phase $\phi(z)$ over region $z = [-3, 3]\delta z$, where $\delta z = 4$ μm is the pixel size in the object space. The evaluated phase distribution is shown in Fig. 8(b).

3. Characterization of imaging resolution

The longitudinal extension of the condensates is $L = 60$–120 μm depending on the total atom number. Because of the random walk of atoms in the imaging light and diffusion of emitted photons, the effective imaging resolution is larger than the imaging resolution δz. The effective imaging resolution is critical for the evaluation of the local number squeezing factor. We show in Fig. 9 that the calculated ξ_N^2 reaches a steady value with integration regions above 28 μm. This length signifies the effective resolution which is still a few times smaller than the condensate length.

4. Mean-field Josephson oscillation

We show in Fig. 10 an example of Josephson oscillation of relative imbalance $\langle n_p \rangle$ by imprinting an initial nonzero imbalance, which is used for extraction of the plasma frequency f_p [shown in Fig. 6(c)].

For comparison, we also display the typical evolution of the imbalance, $\langle n_\xi \rangle \approx 0$, in the case of symmetric splitting investigated in this work.

5. Fit and error bars

Squeezing oscillations are fitted with the function $\xi^2(t) = a\sin(2\pi f_\xi \cdot t + p_0) + \overline{\xi^2}$, with a, f_ξ, p_0, and $\bar{\xi}$ as its fit parameters. The shaded region of the fitted model in Figs. 3, 4, and 5(a) signifies 68% simultaneous bound prediction confidence intervals of the fit function. Error bars on experimentally measured squeezing factors are estimated standard error using a jackknife resampling.

6. Semiclassical simulation on squeezing oscillations

To visualize the squeezing oscillation in the coupled DW (see Fig. 3), we set up a semiclassical simulation. In Fig. 11, we plot the equipotential lines in the classical phase space given by the two-mode Bose-Hubbard model,

$$\mathcal{H} = \frac{2J}{\hbar}\left[\frac{\Lambda}{2}n^2 - \sqrt{1 - n^2}\cos\Phi\right], \tag{A2}$$

where $\Lambda = UN/2J$ signifies the interplay between the interatomic interaction energy and tunnel coupling energy.

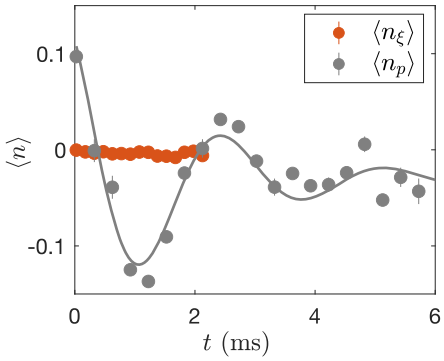

FIG. 10. Evolution of expectation value of relative imbalance $\langle n \rangle = \langle N_-/N \rangle$ in coupled DW. Gray markers, $\langle n_p \rangle$, show Josephson oscillation with an imprinted nonzero initial imbalance. Orange markers, $\langle n_\xi \rangle$, indicate that the expectation values are at equilibrium after symmetrical splitting.

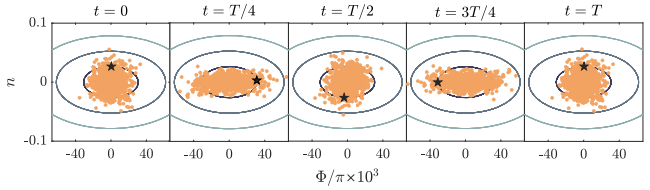

FIG. 11. Propagation of imprinted initial fluctuations in the two-mode BH model. The star marker signifies the evolution of a single realization, representing the mean-field value. A π rotation of a single realization corresponds to a 2π rotation of the phase space fluctuations. Here T is one period of Josephson oscillation.

With suitable parameter values for DW $\mathcal{A} = 0.5$: single particle tunnel coupling energy $J = 41$ Hz, interaction energy $U = 0.33$ Hz, and total atom number $N = 3500$. Here J is estimated using the energy difference between the two lowest single particle eigenstates in the simulated DW potential, $J = (E_1 - E_0)/2$, and experimentally measured atom number N.

Around the stable fixed point and given small fluctuations in the lower energy states, the BH Hamiltonian can be further linearized and expressed in harmonic approximation as

$$H_{hc} = \frac{hf_p}{2}\left(\frac{\Phi^2}{2\Delta_{\mathrm{GS}}^2\Phi} + \frac{N_-^2}{2\Delta_{\mathrm{GS}}^2 N_-}\right), \tag{A3}$$

where $\Delta_{\mathrm{GS}}^2\Phi = \sqrt{1+\Lambda}/N$ and $\Delta_{\mathrm{GS}}^2 N_- = N/\sqrt{1+\Lambda}$ are ground state fluctuations. With these parameters, we can estimate the expected ground state squeezing factors in Eq. (A3) to be

$$\xi_{N,0}^2 = 1/\sqrt{1+\Lambda}, \qquad \xi_{\Phi,0}^2 = \sqrt{1+\Lambda}, \tag{A4}$$

shown as shaded bands in Fig. 1(b).

We sample 1000 realizations from two normal distributions (one for each observable) with variances larger than the ground state fluctuations Δ_{GS}^2 [deduced from Eq. (A3)] and propagate them with equations of motion deduced from Eq. (A2) in the classical limit. We show in Fig. 11 the simulation result of quantum state propagation in a time span of $T = 1/f_p$, where T corresponds to a period of Josephson oscillation of the expectation value of the obsevables (star marker). To make this more explicit, we plot the evolution of N_- and Φ of a single realization and the projected fluctuations as squeezing factor ξ^2 in each quadrature in Fig. 12. As one can see, the projection noise in each observable oscillates at twice the frequency as the expectation values, namely $f_\xi = 2f_p$ (see also Ref. [38]).

7. Impact of number squeezing on global phase diffusion

In decoupled trap ($J \approx 0$), phase diffusion after symmetric splitting [49,50] can be expressed as

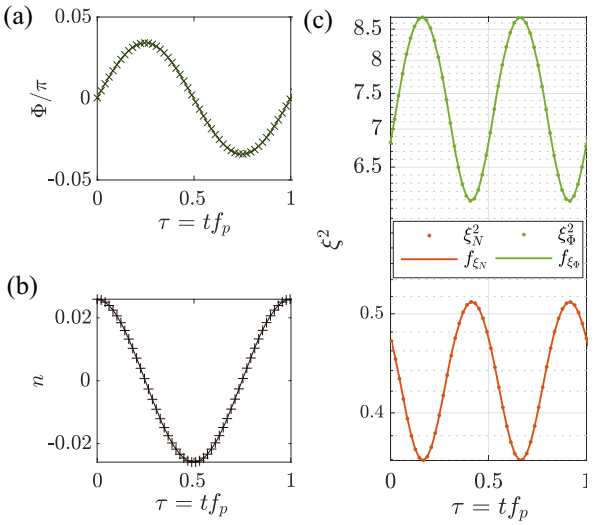

FIG. 12. Squeezing oscillation frequency. Evolution of a single realization in Fig. 11 in the Φ [in (a)] and N_- quadrature [in (b)]. Evolution of quantum fluctuation in the conjugate quadratures [in (c)] and its fitted frequency corresponding to twice the plasma frequency f_p.

$$\Delta^2\Phi(t) = \Delta^2\Phi_0 + R^2t^2, \tag{A5}$$

where $R = (\xi_N\sqrt{N}/\hbar)(\partial\mu/\partial\mathcal{N})|_{\mathcal{N}=N/2}$ is the phase diffusion rate and $\Delta^2\Phi_0$ is the initial variance of Φ right after splitting and $\mu(\mathcal{N})$ is the chemical potential of BEC with atom number $\mathcal{N}$. Equation (A5) implies slower phase diffusion with stronger number squeezing.

We investigate experimentally the influence of number squeezing on global phase diffusion rate by splitting into effectively decoupled DW, $\mathcal{A} = 0.6$. For different split speed $\kappa = \delta\mathcal{A}/\delta t$ we measure the phase spread $\Delta\Phi(t)$ and deduce the phase diffusion rate from a linear fit. The extracted rates $\partial_t\Delta\Phi$ match the trend of the measured ξ_N (see Fig. 13).

8. Impact of number squeezing on spatial dephasing

For resolving local dynamics between two split 1D condensates, we introduce the local observables along the

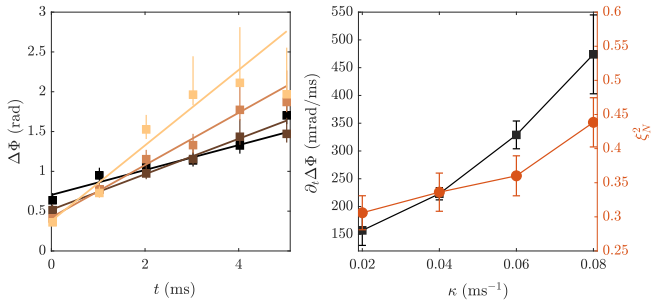

FIG. 13. Global number squeezing suppresses global phase diffusion in decoupled trap. Left: phase diffusion in $\mathcal{A} = 0.6$ trap for different splitting speeds κ. Right: the linearly fitted phase diffusion rates $\partial_t\Delta\Phi$ agree qualitatively with the measured ξ_N with different κ.

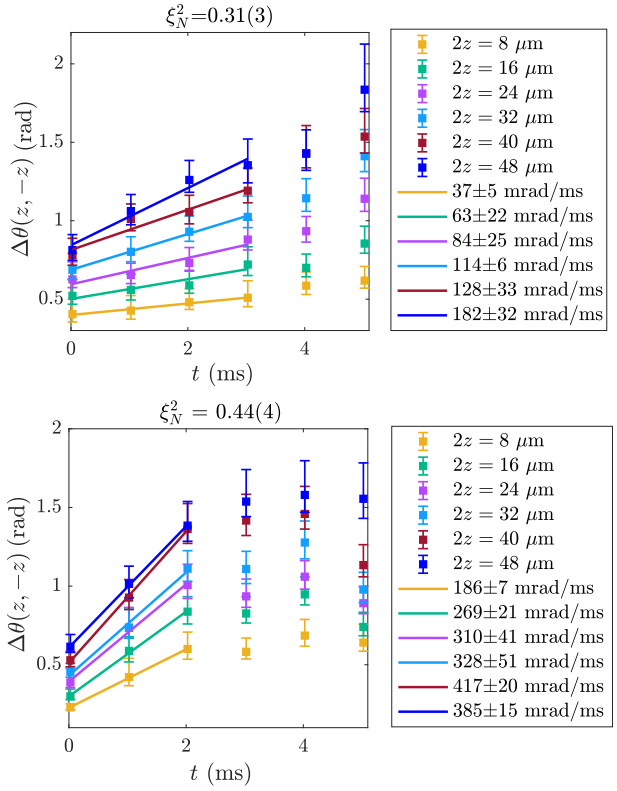

FIG. 14. Extraction of local dephasing rates in decoupled trap in relation to global number squeezing. Evolution of spatial relative phase fluctuations $\Delta\theta(z,-z)$ between two symmetrically located points around the longitudinal center of the BEC. Upper panel: $\Delta\theta(z,-z)$ evolution with global number squeezing $\xi_N^2 = 0.31(3)$ and a linear fit on the four first time instances. Lower panel: $\Delta\theta(z,-z)$ evolution with global number squeezing $\xi_N^2 = 0.44(4)$ and a linear fit on the three first time instances.

condensates: the local relative phase $\phi(z) = \phi_L(z) - \phi_R(z)$ and the relative density $\rho_-(z) = \rho_L(z) - \rho_R(z)$. The local and global observables fulfill the relation $\Phi = \arg\{\overline{\exp[i\phi(z)]}\}$, $N_- = \sum_z \rho_-(z)$.

In previous works studying the phenomenon of prethermalization [26,27], the effective temperature T^- between the two condensates was connected to the relative density fluctuations $\Delta^2\rho_- = \langle\rho_-^2\rangle$ by

$$T^- = \frac{g\Delta^2\rho_-}{2} = \frac{g\rho_0\xi_\rho^2}{2}, \tag{A6}$$

where ρ_0 is the peak atomic density in each condensate after splitting and ξ_ρ^2 is the local number squeezing factor.

[1] L. Pezzè, A. Smerzi, M. K. Oberthaler, R. Schmied, and P. Treutlein, *Quantum metrology with nonclassical states of atomic ensembles*, Rev. Mod. Phys. **90**, 035005 (2018).

[2] V. Giovannetti, S. Lloyd, and L. Maccone, *Quantum-enhanced measurements: Beating the standard quantum limit*, Science **306**, 1330 (2004).

[3] I. Bloch, J. Dalibard, and S. Nascimbene, *Quantum simulations with ultracold quantum gases*, Nat. Phys. **8**, 267 (2012).

[4] O. Gühne and G. Tóth, *Entanglement detection*, Phys. Rep. **474**, 1 (2009).

[5] C. Gross, T. Zibold, E. Nicklas, J. Esteve, and M. K. Oberthaler, *Nonlinear atom interferometer surpasses classical precision limit*, Nature (London) **464**, 1165 (2010).

[6] M. F. Riedel, P. Böhi, Y. Li, T. W. Hänsch, A. Sinatra, and P. Treutlein, *Atom-chip-based generation of entanglement for quantum metrology*, Nature (London) **464**, 1170 (2010).

[7] B. Lücke *et al.*, *Twin matter waves for interferometry beyond the classical limit*, Science **334**, 773 (2011).

[8] C. D. Hamley, C. Gerving, T. Hoang, E. Bookjans, and M. S. Chapman, *Spin-nematic squeezed vacuum in a quantum gas*, Nat. Phys. **8**, 305 (2012).

[9] J. Esteve, C. Gross, A. Weller, S. Giovanazzi, and M. K. Oberthaler, *Squeezing and entanglement in a Bose-Einstein condensate*, Nature (London) **455**, 1216 (2008).

[10] T. Berrada, S. van Frank, R. Bücker, T. Schumm, J.-F. Schaff, and J. Schmiedmayer, *Integrated Mach-Zehnder interferometer for Bose-Einstein condensates* Nat. Commun. **4**, 2077 (2013).

[11] E. Nicklas, M. Karl, M. Hofer, A. Johnson, W. Muessel, H. Strobel, J. Tomkovic, T. Gasenzer, and M. K. Oberthaler, *Observation of scaling in the dynamics of a strongly quenched quantum gas*, Phys. Rev. Lett. **115**, 245301 (2015).

[12] A. Farolfi, A. Zenesini, R. Cominotti, D. Trypogeorgos, A. Recati, G. Lamporesi, and G. Ferrari, *Manipulation of an elongated internal Josephson junction of bosonic atoms*, Phys. Rev. A **104**, 023326 (2021).

[13] M. Pigneur, T. Berrada, M. Bonneau, T. Schumm, E. Demler, and J. Schmiedmayer, *Relaxation to a phase-locked equilibrium state in a one-dimensional bosonic Josephson junction*, Phys. Rev. Lett. **120**, 173601 (2018).

[14] V. Gritsev, A. Polkovnikov, and E. Demler, *Linear response theory for a pair of coupled one-dimensional condensates of interacting atoms*, Phys. Rev. B **75**, 174511 (2007).

[15] S. Coleman, *Quantum sine-Gordon equation as the massive Thirring model*, Phys. Rev. D **11**, 2088 (1975).

[16] T. Schweigler, V. Kasper, S. Erne, I. Mazets, B. Rauer, F. Cataldini, T. Langen, T. Gasenzer, J. Berges, and J. Schmiedmayer, *Experimental characterization of a quantum many-body system via higher-order correlations*, Nature (London) **545**, 323 (2017).

[17] T. Schweigler *et al.*, *Decay and recurrence of non-Gaussian correlations in a quantum many-body system*, Nat. Phys. **17**, 559 (2021).

[18] G.-S. Paraoanu, S. Kohler, F. Sols, and A. Leggett, *The Josephson plasmon as a Bogoliubov quasiparticle*, J. Phys. B **34**, 4689 (2001).

[19] A. Smerzi, S. Fantoni, S. Giovanazzi, and S. Shenoy, *Quantum coherent atomic tunneling between two trapped Bose-Einstein condensates*, Phys. Rev. Lett. **79**, 4950 (1997).

[20] S. Raghavan, A. Smerzi, S. Fantoni, and S. Shenoy, *Coherent oscillations between two weakly coupled Bose-Einstein condensates: Josephson effects, π oscillations, and*

macroscopic quantum self-trapping, Phys. Rev. A **59**, 620 (1999).

[21] M. Albiez, R. Gati, J. Folling, S. Hunsmann, M. Cristiani, and M. K. Oberthaler, *Direct observation of tunneling and nonlinear self-trapping in a single bosonic Josephson junction*, Phys. Rev. Lett. **95**, 010402 (2005).

[22] R. Gati and M. K. Oberthaler, *A bosonic Josephson junction*, J. Phys. B **40**, R61 (2007).

[23] S. Levy, E. Lahoud, I. Shomroni, and J. Steinhauer, *The ac and dc Josephson effects in a Bose-Einstein condensate*, Nature (London) **449**, 579 (2007).

[24] L. J. LeBlanc, A. B. Bardon, J. McKeever, M. H. T. Extavour, D. Jervis, J. H. Thywissen, F. Piazza, and A. Smerzi, *Dynamics of a tunable superfluid junction*, Phys. Rev. Lett. **106**, 025302 (2011).

[25] G. Spagnolli *et al.*, *Crossing over from attractive to repulsive interactions in a tunneling bosonic Josephson junction*, Phys. Rev. Lett. **118**, 230403 (2017).

[26] T. Kitagawa, A. Imambekov, J. Schmiedmayer, and E. Demler, *The dynamics and prethermalization of one-dimensional quantum systems probed through the full distributions of quantum noise*, New J. Phys. **13**, 073018 (2011).

[27] M. Gring, M. Kuhnert, T. Langen, T. Kitagawa, B. Rauer, M. Schreitl, I. Mazets, D. Adu Smith, E. Demler, and J. Schmiedmayer, *Relaxation and prethermalization in an isolated quantum system*, Science **337**, 1318 (2012).

[28] J. Reichel and V. Vuletic, *Atom Chips* (John Wiley & Sons, New York, 2011).

[29] S. Hofferberth, I. Lesanovsky, B. Fischer, J. Verdu, and J. Schmiedmayer, *Radiofrequency-dressed-state potentials for neutral atoms*, Nat. Phys. **2**, 710 (2006).

[30] R. Bücker, A. Perrin, S. Manz, T. Betz, Ch. Koller, T. Plisson, J. Rottmann, T. Schumm, and J. Schmiedmayer, *Single-particle-sensitive imaging of freely propagating ultracold atoms*, New J. Phys. **11**, 103039 (2009).

[31] Y. Castin and J. Dalibard, *Relative phase of two Bose-Einstein condensates*, Phys. Rev. A **55**, 4330 (1997).

[32] K. Maussang, G. E. Marti, T. Schneider, P. Treutlein, Y. Li, A. Sinatra, R. Long, J. Esteve, and J. Reichel, *Enhanced and reduced atom number fluctuations in a BEC splitter*, Phys. Rev. Lett. **105**, 080403 (2010).

[33] G.-B. Jo, Y. Shin, S. Will, T. A. Pasquini,M. Saba, W. Ketterle, D. E. Pritchard, M. Vengalattore, and M. Prentiss, *Long phase coherence time and number squeezing of two Bose-Einstein condensates on an atom chip*, Phys. Rev. Lett. **98**, 030407 (2007).

[34] D. J. Wineland, J. J. Bollinger, W. M. Itano, and D. Heinzen, *Squeezed atomic states and projection noise in spectroscopy*, Phys. Rev. A **50**, 67 (1994).

[35] A. Sørensen, L.-M. Duan, J. I. Cirac, and P. Zoller, *Many-particle entanglement with Bose-Einstein condensates*, Nature (London) **409**, 63 (2001).

[36] G. Milburn, J. Corney, E. M. Wright, and D. Walls, *Quantum dynamics of an atomic Bose-Einstein condensate in a double-well potential*, Phys. Rev. A **55**, 4318 (1997).

[37] M. Lewenstein and L. You, *Quantum phase diffusion of a Bose-Einstein condensate*, Phys. Rev. Lett. **77**, 3489 (1996).

[38] J. Dunningham, K. Burnett, and M. Edwards, *Relative number squeezing in Bose-Einstein condensates*, Phys. Rev. A **64**, 015601 (2001).

[39] G. Jäger, T. Berrada, J. Schmiedmayer, T. Schumm, and U. Hohenester, *Parametric-squeezing amplification of Bose-Einstein condensates*, Phys. Rev. A **92**, 053632 (2015).

[40] J. Grond, G. von Winckel, J. Schmiedmayer, and U. Hohenester, *Optimal control of number squeezing in trapped Bose-Einstein condensates*, Phys. Rev. A **80**, 053625 (2009).

[41] L. Xin, M. Chapman, and T. Kennedy, *Fast generation of time-stationary spin-1 squeezed states by nonadiabatic control*, PRX Quantum **3**, 010328 (2022).

[42] L. Xin, M. Barrios, J. T. Cohen, and M. S. Chapman, *Long-lived squeezed ground state in a spin-1 Bose-Einstein condensate*, Phys. Rev. Lett. **131**, 133402 (2023).

[43] I. Lovas, R. Citro, E. Demler, T. Giamarchi, M. Knap, and E. Orignac, *Many-body parametric resonances in the driven sine-Gordon model*, Phys. Rev. B **106**, 075426 (2022).

[44] S.-C. Ji, T. Schweigler, M. Tajik, F. Cataldini, J. Sabino, F. S. Moller, S. Erne, and J. Schmiedmayer, *Floquet engineering a bosonic Josephson junction*, Phys. Rev. Lett. **129**, 080402 (2022).

[45] R. Bistritzer and E. Altman, *Intrinsic dephasing in one-dimensional ultracold atom interferometers*, Proc. Natl. Acad. Sci. U.S.A. **104**, 9955 (2007).

[46] S. A. Erne, *Far-from-Equilibrium Quantum Many-Body Systems: From Universal Dynamics to Statistical Mechanics*, Ph.D. thesis, Heidelberg University, 2018, http://www.ub.uni-heidelberg.de/archiv/25106.

[47] T. Langen, S. Erne, R. Geiger, B. Rauer, T. Schweigler, M. Kuhnert, W .Rohringer, I. E. Mazets, T. Gasenzer, and J. Schmiedmayer, *Experimental observation of a generalized Gibbs ensemble*, Science **348**, 207 (2015).

[48] M. Tajik *et al.*, *Experimental verification of the area law of mutual information in quantum field simulator*, Nat. Phys. **19**, 1022 (2023).

[49] J. Javanainen and M. Wilkens, *Phase and phase diffusion of a split Bose-Einstein condensate*, Phys. Rev. Lett. **78**, 4675 (1997).

[50] A. Leggett and F. Sols, *Comment on "Phase and phase diffusion of a split Bose-Einstein condensate,"* Phys. Rev. Lett. **81**, 1344 (1998).